Molecular Therapy
Nucleic Acids
Original Article

A Deoxyribonucleic Acid Decoy Trapping DUX4 for the Treatment of Facioscapulohumeral Muscular Dystrophy

Virginie Mariot,[1] Romain Joubert,[1] Anne-Charlotte Marsollier,[1] Christophe Hourdé,[2] Thomas Voit,[1] and Julie Dumonceaux[1,3]

[1]NIHR GOSH Biomedical Research Centre, University College London, Great Ormond Street Institute of Child Health and Great Ormond Street Hospital NHS Trust, London WC1N 1EH, UK; [2]Inter-University Laboratory of Human Movement Biology (LIBM), EA7424 Université Savoie Mont Blanc, Campus Scientifique Technolac, 73376 Le Bourget du Lac Cedex, France; [3]Northern Ireland Center for Stratified/Personalised Medicine, Biomedical Sciences Research Institute, Ulster University, Derry/Londonderry BT47 6SB, Northern Ireland, UK

Facioscapulohumeral dystrophy (FSHD) is characterized by a loss of repressive epigenetic marks leading to the aberrant expression of the DUX4 transcription factor. In muscle, DUX4 acts as a poison protein though the induction of multiple downstream genes. So far, there is no therapeutic solution for FSHD. Because DUX4 is a transcription factor, we developed an original therapeutic approach, based on a DNA decoy trapping the DUX4 protein, preventing its binding to genomic DNA and thereby blocking the aberrant activation of DUX4's transcriptional network. *In vitro*, transfection of a DUX4 decoy into FSHD myotubes reduced the expression of the DUX4 network genes. *In vivo*, both double-stand DNA DUX4 decoys and adeno-associated viruses (AAVs) carrying DUX4 binding sites reduced transcriptional activation of genes downstream of DUX4 in a DUX4-expressing mouse model. Our study demonstrates, both *in vitro* and *in vivo*, the feasibility of the decoy strategy and opens new avenues of research.

INTRODUCTION

Facioscapulohumeral dystrophy (FSHD, OMIM 158900)[1] is one of the most common muscular dystrophies. FSHD onset is usually in teenage or early adult years and the disease progresses slowly (for review see Wagner[2]) The major symptoms are a rapid loss of selected muscles, including the muscles of the face, the shoulder, and the upper arm. So far there is no curative or preventive treatment. The genetic basis of the disease has been recently elucidated: FSHD is characterized by a loss of repressive epigenetic marks within the D4Z4 array located on the subtelomeric part of chromosome 4, leading to chromatin relaxation and, when associated with a permissive chromosome 4, to the expression of the normally silenced DUX4 protein[3] whose open reading frame (ORF) is present in each D4Z4 repeat.[4,5] DUX4 is a transcription factor resulting in a poison protein through induction of downstream genes.[1,6] DUX4 expression is extremely low but it has been robustly found in adult and fetal FSHD muscle cells and biopsies.[3,7–9] DUX4 might be the major trigger of FSHD onset/progression by disrupting several cellular pathways and inducing cell death in different models (for review see DeSimone et al.[10]). Several laboratories, including ours, have developed therapeutic strategies based on DUX4 silencing mediated by RNA interference, antisense oligonucleotides (AONs), artificial miRNAs, the short-spliced form of DUX4 (DUX4 s), or drugs.[11–19]

In this study, we describe a new strategy based on a DUX4 decoy. DUX4 is a transcription factor, and DUX4 binding sites have been previously identified.[6,20] They include the minimum sequences of the DUX4 binding motif in non-repetitive elements and MaLR-associated sites, which are TAAYYBAATCA and TAAYBYAATCA, respectively (according to International Union of Pure and Applied Chemistry [IUPAC] nomenclature). We sought to develop a DNA decoy-based therapy strategy by trapping the endogenous DUX4, thereby preventing its binding to genomic DNA and thereby blocking transcriptional activation of genes downstream of DUX4.

RESULTS

DUX4 Decoys Reduce Transcriptional Activation of Genes Downstream of DUX4 *In Vitro*

The 5′-TAATCCAATCA-3′ DUX4 binding motif, previously described to bind DUX4 in an electromobility shift assay (EMSA),[6] was used to design six double-strand oligonucleotide DNA decoys. They differ in their structures (linear or circular), chemical modifications (presence or not of phosphorothioate links and/or hexaethylene glycol linkage [18-HEG]), or lengths (Figure 1A). Their capacity to inhibit DUX4 action was explored after transfection into FSHD myotubes, and the expression levels of three well-characterized DUX4 downstream genes were analyzed. All of the constructs were able to diminish ZSCAN4 and TRIM43 expression (9%–61% mRNA left)

Received 2 April 2020; accepted 13 October 2020;
https://doi.org/10.1016/j.omtn.2020.10.028.

Correspondence: Julie Dumonceaux, PhD, NIHR GOSH Biomedical Research Centre, University College London, Great Ormond Street Institute of Child Health and Great Ormond Street Hospital NHS Trust, 30 Guilford Street, London WC1N 1EH, UK.
E-mail: j.dumonceaux@ucl.ac.uk

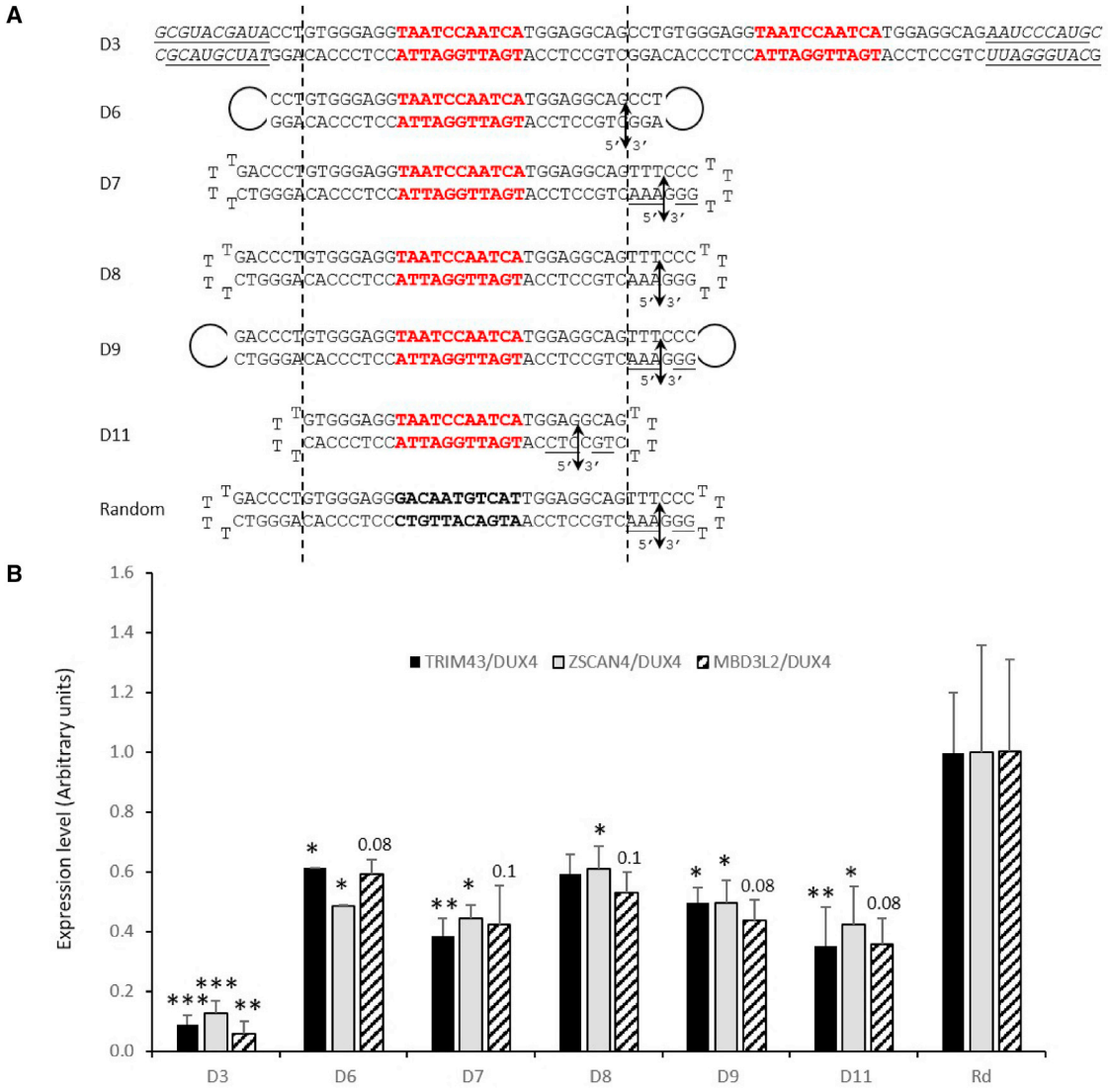

Figure 1. Decoys Targeting DUX4 Protein Are Able to Decrease DUX4-Induced Gene Activation *In Vitro*

(A) Design of the different decoys used. The sequence in-between the dashed line is common to all of the decoys except for the random decoy. The DUX4 binding site is in red. The random sequence (generated by the random DNA sequence generator, the percentage of GC was conserved; http://www.faculty.ucr.edu/~mmaduro/random.htm) is bolded. The decoys are two oligonucleotides that are hybridized together (decoy 3 [D3]) or double-strand DNA synthetized as one single DNA strand (D6–D11 and random), which are ligated before transfection. Chemical modifications are as follows: italic indicates 2′-*O*-methyl bases; underlined bases carry a phosphorothioate linkage; the hexaethylene glycol linkers are represented by gray brackets; the minimal DUX4 binding sites are in bold; and arrows indicate the junction between the beginning and the end of the oligonucleotide before ligation. (B) FSHD myoblasts were transfected with the different decoys, and the levels of genes downstream of DUX4 were performed, normalized to *DUX4* expression. *GAPDH* was used as a normalizer. The data represent mean ± SEM from at least four independent experiments. *$p < 0.05$, **$p < 0.01$ determined by an ANOVA test followed by a Newman-Keuls post hoc test. Rd, random.

compared to a random decoy (Figure 1B). D3 appeared to be the best decoy but its transfection was associated with a high toxicity, with cells detaching within the days following transfection. For MBD3L2, decoys D6–D11 led to a decrease (from 36% ± 9% to 59% ± 5% mRNA left) with a statistical significance from 0.08 to 0.1.

Using a univariate test of significance, followed by a Newman-Keuls post hoc test, we analyzed the different properties of the decoys. We did not see differences between the different decoys even if D7 and D11, which carry phosphorothioate links but no hexaethylene glycol linkage, seemed to give the best results.

Double-Stand DNA DUX4 Decoys Reduce Transcriptional Activation of Genes Downstream of DUX4 *In Vivo*

As a next step toward translation, *in vivo* testing of potential therapeutic decoys was realized. A DUX4 expression plasmid (pCS2) was

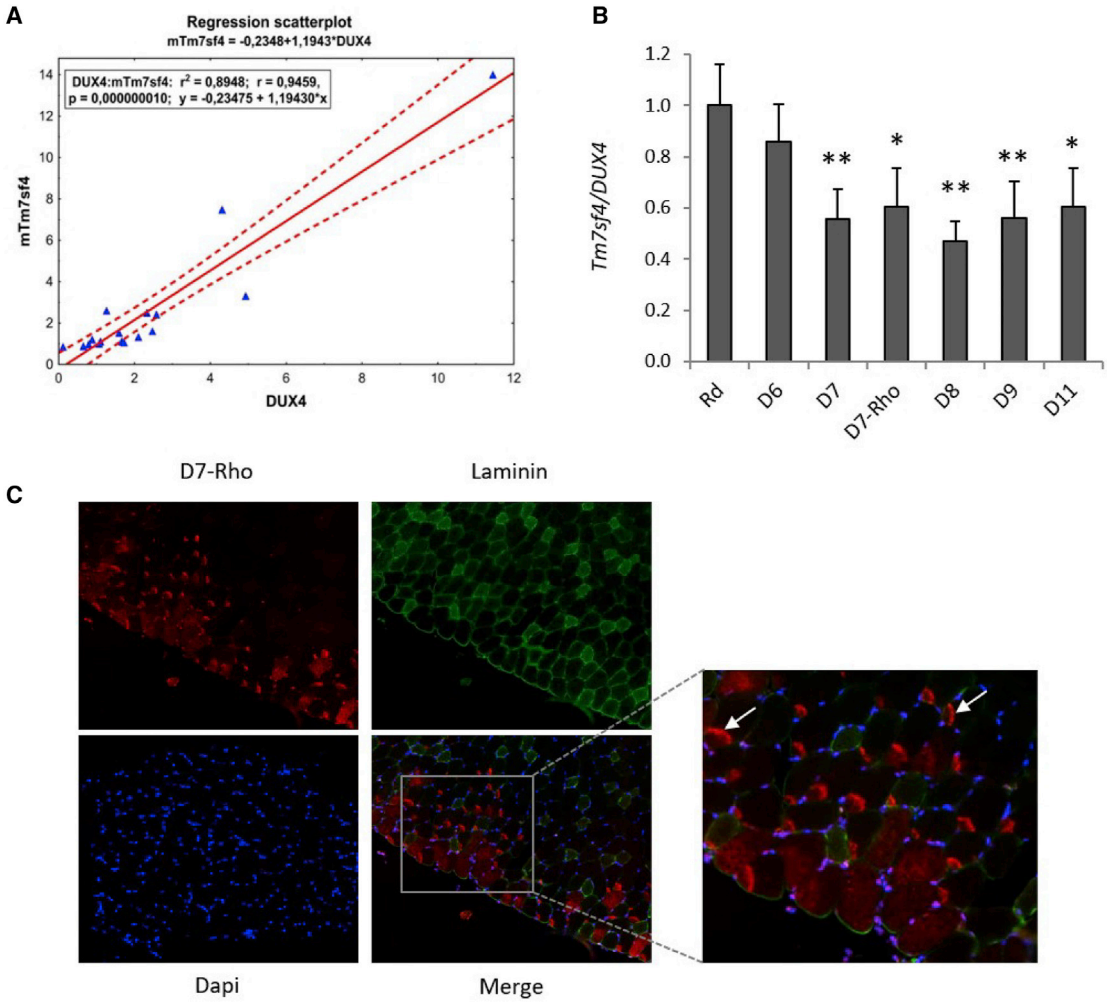

Figure 2. Oligonucleotide-Based Decoys Inhibit DUX4-Induced Gene Transcription *In Vivo*

(A and B) *Tibiales anterior* (TAs) of C57BL/6 mice were electrotransferred with the pCS2 plasmid coding for DUX4 in the presence of the different decoys. Expression levels of both *DUX4* and *Tm7sf4* mRNAs were analyzed by qPCR since a multiparametric analysis of variance (MANOVA) and a Newman-Keuls post hoc test had revealed a strong correlation between DUX4 and *Tm7sf4* (A) ($r^2 = 0.8948$, p = 10e−8). Mice were sacrificed 4 days after injection and total RNA was extracted. The histograms represent *Gapdh* normalized data (B). At least eight TAs were analyzed per group. Data are presented as the mean ± SEM of three or more independent experiments. *p < 0.05, **p < 0.01, by one-way ANOVA. (C) Decoy 7 carrying a rhodamine (Rho) fluorescence decoy was electrotransferred into the TA of C57BL/6 mice. Four days later, mice were sacrificed and muscles were sectioned (8 μm). The D7-Rho is seen in red, the laminin is labeled in green using a polyclonal rabbit anti-laminin antibody (Z0097, Dako, Les Ulis, France), and nuclei are counterstained in blue using DAPI. In the merged image, examples of decoy accumulation in the fibers are indicated by arrows. Images from muscle without fluorescent-labeled decoy are presented in Figure S1.

intramuscularly electrotransferred into the *tibialis anterior* (TA) of C57BL/6 mice. As electrotransfer efficiency might vary between mice, inducing a variation in DUX4 levels independently of the presence of decoys, a statistical correlation between DUX4 expression and the DUX4 target gene *Tm7sf4*[21] was first established ($r^2 = 0.89$) (Figure 2A). Decoys were intramuscularly electrotransferred in the presence of the pCS2 plasmid. In order to avoid any bias relative to electrotransfer efficiency and because the decoy mechanism of action is to trap DUX4 without impacting *DUX4* mRNA expression, the decoy efficacies were analyzed by calculating the expression level of *Tm7sf4* relative to *DUX4*. We observed a 40%–53% reduction in the presence of the decoys (with the exception of D6) compared to a random sequence decoy (Figure 2B). This demonstrates that most of the decoys, once transfected into muscle fibers, are stable enough to trap DUX4, diminish its binding to genomic DNA sequences, and consequently inhibit the activation of genes downstream of DUX4. Subcellular distribution of the decoy as well as its presence at the time of sacrifice have been documented through electrotransfer of a rhodamine-labeled D7 decoy (D7-Rho) with an identical efficacy to the native D7 decoy (Figures 2B and 2C). The D7-Rho localized to the cytoplasm of muscle fibers as expected (Figure 2C).

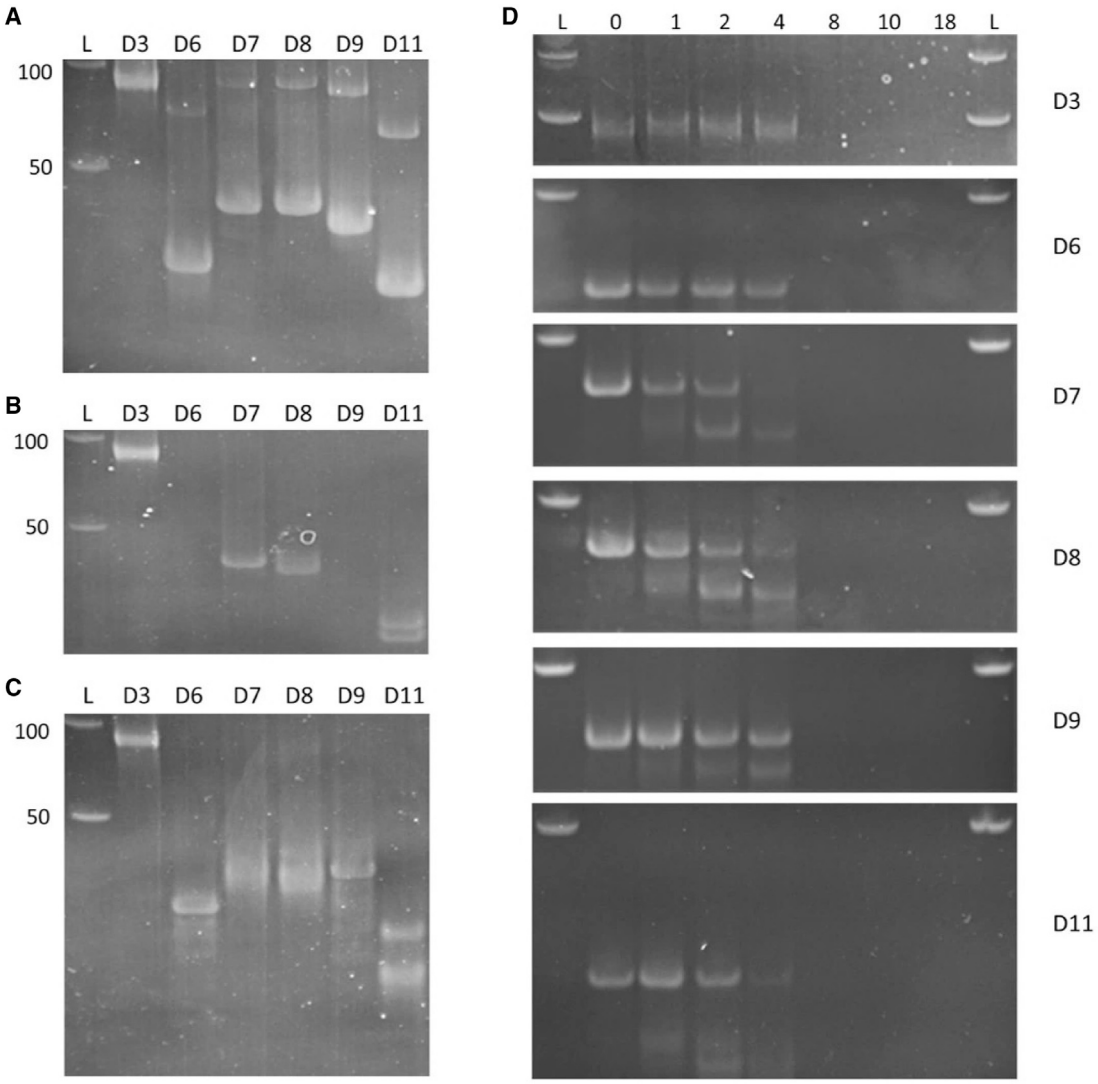

Figure 3. Molecular Stability of the DNA Decoys in the Presence of Nucleases

(A–D) Decoys were incubated in the presence of differentiation medium (A), exonuclease III (B), nuclease S1 (C), or FBS for 0, 1, 2, 4, 8, 10, or 18 h (D) and loaded on a 15% acrylamide gel. L, 50-bp ladder. D3–D11 indicate the different decoys. Lengths of the double strands: D3, 82 bp; D6, 34 bp; D7, D8, and D9, 40 bp; D11, 28 bp.

Decoy Stability

We next investigated decoy stability under conditions mimicking systemic delivery. The molecular stability of the DNA decoys was thus examined in the presence of nucleases. In differentiation medium, all (with the exception of D3) decoys showed high molecular weights (Figure 3A), which might correspond to concatemerized forms and which disappear in the presence of nucleases (Figures 3B and 3C). By exonuclease III, decoys D6 and D9 are totally degraded (Figure 3B). Because exonuclease III catalyzes the stepwise removal of mononucleotides starting from a 3′-OH at nicks and blunt ends in double-strand DNA, the presence of the hexaethylene glycol may have affected the ligation efficiency, leading to the formation of nicks (Figure 3B). In the presence of nuclease S1, which preferentially degrades single-strand DNA, D7, D8, and D11 presented lower molecular weights, thus suggesting that the TTTT single-strand loop triggers the degradation (Figure 3C). Finally, all of the decoys were degraded after 8-h treatment in fetal bovine serum (FBS) (Figure 3D), but the presence of the hexaethylene glycol led to a stronger resistance to nucleases (D6 and D9, Figure 3D).

AAVs Carrying DUX4 Binding Sites Reduce Transcriptional Activation of Genes Downstream of DUX4 *In Vivo*

We thus decided to create an adeno-associated virus (AAV) vector carrying two DUX4 decoy sequences (AAV-decoy). TA muscles of C57BL/6 mice were transduced with either AAV-decoy or an AAV-control (AAV-GFP) 14 days before the pCS2 electrotransfer, and the expression levels of several murine genes downstream of

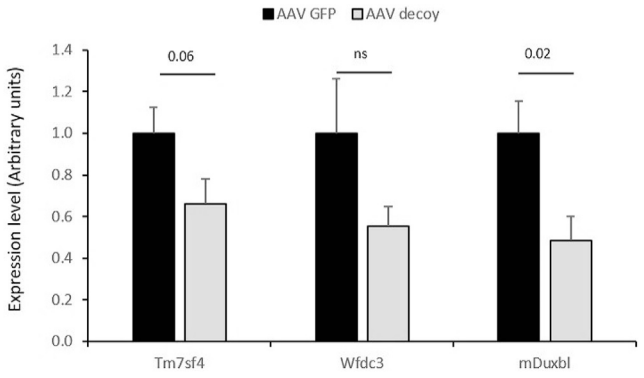

Figure 4. AAV-Based Decoys Inhibit DUX4-Induced Gene Transcription *In Vivo*

TAs of C57BL/6 mice were injected with 2.5e10 vg/TA of AAV-GFP or AAV-decoy (35 μL). 14 days later, the pCS2 plasmid was electrotransferred into the muscles. Mice were sacrificed 4 days later and total RNA was extracted and expression levels of *DUX4* and *Tm7sf4*, *wfdc3*, and *Duxbl* were analyzed by qPCR. The boxplots were normalized using *Gapdh*. Data are presented as the mean ± SEM of three or more independent experiments ($n \geq 8$ TAs/group). *$p < 0.05$, by a t test.

DUX4[21] were analyzed. A 34% decrease ($p = 0.066$) of the *Tm7sf4/DUX4* ratio was observed in the presence of AAV-decoy, as well as a 51% ($p = 0.02$) fold decrease for *DuxBl* (Figure 4). *Wfdc3* remained unchanged ($p = 0.14$). This result demonstrated the ability of the AAV-decoy vector to inhibit DUX4-mediated activation of *Tm7sf4*.

DISCUSSION

During the past two decades, many noncoding oligonucleotide strategies have been developed to modify gene expression through repression or activation of a specific pathway, including small interfering RNAs to silence gene expression, antisense oligonucleotides to reduce protein translation, RNA decoys to compete with natural targets, or ribozymes to cleave mRNAs (for review see Shum and Rossi[22]). In this study, we developed a double-strand deoxyribonucleic acid decoy *cis*-element to block the binding of DUX4 to its genomic DNA target sequences. One of our decoys (D3) was toxic after transfection in muscle cells. D3 carries phosphorothioate linkages, which improve oligonucleotide stabilization and internalization in most cells in a sequence-independent, but length-dependent, binding to several cellular proteins, including laminin and fibronectin.[23] However, phosphorothioates are also toxic due to their non-specific binding to proteins,[24] and this could explain the D3-mediated toxicity. We established a proof of principle for this therapeutic strategy capable of being delivered at a level significant enough to treat skeletal muscle pathology intramuscularly.

One important question regards the potential side effects of this approach. The decoy does not require any promoter to be effective and does not encode a message by itself. However, DUX4 and PAX3/7 binding sites are very close, and it was previously demonstrated that Pax3 and Pax7 compete with DUX4 after overexpression of DUX4 in C2C12 cells,[25] and substitution mutants in which DUX4 homeodomains are replaced by Pax7 homeodomains retain the ability to inhibit differentiation and to induce cytotoxicity after overexpression.[26] PAX7 target genes are globally repressed in FSHD muscle biopsies.[27,28] However, DUX4 and PAX7 expressions are spatiotemporally different: DUX4 is rather expressed in myofibers than in myoblasts,[8] and PAX7 is expressed in both quiescent and activated satellite cells before being downregulated to allow cell differentiation.[29] Because AAV vectors do not efficiently target muscle satellite cells,[30] an interaction between the decoy and PAX7 is not likely. As it was previously demonstrated that phosphorodiamidate morpholino oligomer (PMO)-based antisense oligonucleotides can be found in PAX7-expressing satellite cells after intravenous injections,[31] an AAV-based therapeutic approach would be privileged over a nucleotide-based decoy. Moreover, AAV-based therapy has the potential to provide long-lasting, one-time treatment.

Another important point is the location of the decoy within muscle fibers. DUX4 being a transcription factor, it is mainly located within the nucleus, and our study has shown that oligonucleotide-based decoys are mostly located within the cytoplasm. However, we have previously demonstrated that once translated, DUX4 protein is able to diffuse into nearby nuclei within myotubes,[1] thus demonstrating its presence also in the cytoplasm. The oligonucleotide-based decoys may therefore bind the DUX4 protein during its cytoplasmic phase. This might be very important for the efficiency of this therapeutic approach because in contrast to antisense approaches directed to DUX4 silencing, which needs to target all nuclei of a myofiber in order to suppress DUX4 protein synthesis and in consequence needs high intra-fiber levels, a decoy-based approach with a cytoplasmic distribution will intercept the DUX4 protein irrespective of the nuclei that are involved in DUX4 synthesis. However, AAV-based decoys may trap the DUX4 protein directly within the nuclei because AAV genomes are located in the nucleus.

These observations lead to a crucial question: how can the decoys trap the DUX4 protein, assuming that the human genome may contain hundreds of DUX4 binding sites? The sequence of the decoy we chose, which is one of the strongest DUX4 binding sequences according to a recent study,[20] or the fact that AAV genomes remain primarily episomal after transduction may be part of the answer, which still needs to be deciphered. However, several articles have already described double-strand oligonucleotide decoy-based approaches for other transcription factors, among them E2F,[32,33] STAT3,[34,35] or nuclear factor κB,[36,37] to treat a wide range of diseases such as liver fibrosis, acute myeloid leukemia, myocardial infraction, or ovarian cancer, and a trial of a STAT3 decoy oligonucleotide in head and neck cancer has been already performed.[38] These results demonstrate that targeting a transcription factor using a double-strand oligonucleotide is a viable and safe therapeutic approach to treat several diseases where transcription factors are involved in the pathogenesis. FSHD is a particularly suited disease for this approach because DUX4 is produced at a very low level, which facilitates its neutralization in quantitative terms.

Further studies are now required to systemically inject the decoy in DUX4-expressing mice. Several hurdles will need to be overcome, including an efficient delivery in the body's largest organ, an AAV pre-existing immunity,[39] and an immune response triggered by the AAV vectors,[40] but many laboratories are looking for solutions such as an AAV-specific plasmapheresis column or immunoglobulin G (IgG)-cleaving endopeptidases to reduce anti-AAV antibodies.[41,42]

Overall, our study provides the proof of principle for a new therapeutic approach for FSHD, based on deoxyribonucleic acid decoy, an approach never developed for a neuro-muscular disease before.

MATERIALS AND METHODS

Cell Culture

Primary FSHD1 cells were derived from biopsies as previously described,[8] and the myogenicity was determined by CD56 labeling. The cells were enriched in $CD56^+$ cells using a magnetic-activated cell sorting (MACS) column when the percentage was below 85%. Cells were cultivated in proliferation medium (4 vol of DMEM, 1 vol of 199 medium, 20% FBS, 50 μg/mL gentamycin [Life Technologies, Saint-Aubin, France]) supplemented with 5 μg/mL insulin, 0.2 μg/mL dexamethasone, 0.5 ng/mL basic fibroblast growth factor (bFGF), 5 ng/mL human epidermal growth factor (hEGF), and 25 μg/mL fetuin. Differentiation was induced by replacing the proliferation medium by DMEM supplemented with insulin (10 μg/mL). For D3 decoy, forward and reverse oligonucleotides were annealed at equimolar concentration in a final volume of 50 μL and heated at 95°C for 4 min. For all other decoys, naked oligonucleotides were hybridized. Briefly, 10 μg of decoy was heated at 95°C for 4 min and the temperature was decreased to 20°C with a ramping of 1% using a Veriti thermal cycler (Applied Biosystems). The ligation was performed overnight with the T4 ligase according to the manufacturer's protocol (Life Technologies, Saint-Aubin, France).

Cells were seeded in six-well plates 72 h before differentiation. Transfections were realized at day 2 of differentiation using Lipofectamine RNAiMAX[8] reagent according to the manufacturer's protocol (Invitrogen) with a ratio of 1:5 between DNA and RNAiMAX (the final concentration for the decoy oligonucleotide DNA was 50 nM). Cells were collected 2 days after transfection, which corresponds to day 4 of differentiation, when the picture of DUX4 expression is the highest.[8]

Viral Production

Oligonucleotides for the decoy D3 were cloned into an pGG2 backbone, using the restriction enzymes XbaI and HpaI, leading to the AAV-decoy backbone. All of the vectors were produced in human embryonic kidney 293 cells using polyethylenimine (PEI) (1 mg/mL) by triple transfection at a DNA/PEI ratio of 1:3. The transfected plasmids are pXX6 plasmid coding for the adenoviral sequences essential for AAV production, the pREpCap plasmid coding the AAV-1 capsid, and the viral genome carrying the decoy sequences. Three days after transfection, the supernatant was withdrawn and the collected virus was purified by iodixanol gradient and concentrated by Amicon Ultra-15 columns (Merck Millipore, Molsheim, France).

RNA Extraction and RT-PCR

Total RNAs from either cells or murine muscles were extracted using TRIzol according to the manufacturer's protocol (Life Technologies, Saint-Aubin, France). The reverse transcription, PCR, and qPCR methods were described previously.[43] The primers are described in Table 1. The qPCR Minimum Information for Publication of Quantitative Real-Time PCR Experiments (MIQE) standards were followed.[44] To determine the best reference gene *in vivo*, six different reference genes (*Gapdh*, *Gus*, *Actin*, *Hprt1*, *Cyclophilin*, and *Psma2*) were tested and *Gapdh* was validated as a reference gene for which Ct values were not impacted by the electrotransfer of the decoys. Each PCR product was loaded in a 2% agarose gel and cloned into TOPO TA cloning (Life Technologies, Saint-Aubin, France) and sequenced.

Muscle Injection

All research was conducted according to the French and European regulations and was approved by the French Ministry of Education, Higher Education and Research (agreement no. APAFIS#5555-20l60627l3055186 v3). Injections in the TA were performed on 6- to 8-week-old female C57BL/6 mice. After intraperitoneal anesthesia (100 mg/kg ketamine, 10 mg/kg xylazine), the TA was injected with a mix containing 10 μg of decoy and 2 μg of DUX4 plasmid expression pCS2-mkgDUX4, a gift from Stephen Tapscott (Addgene plasmid no. 21156; http://n2t.net/addgene:21156; RRID: Addgene_21156) in 40 μL of PBS-water (1:1). Transcutaneous electrical pulses were applied by two stainless steel external plate electrodes (Tweezertrodes [7 mm], BTX/Harvard Apparatus), and eight square-wave electric pulses of 200 V/cm and 20-ms duration were generated at 500-ms intervals by a Gentronix BTX ECM830 instrument (BTX/Harvard Apparatus). The AAV-decoy was injected at 2.5×1010 viral genomes (vg)/TA.

Histological Analysis

Mice were euthanized 4 days following electrotransfer and muscles were dissected immediately, two-thirds of TA was mounted in OCT and frozen in isopentane cooled in liquid nitrogen, and one-third was directly frozen in liquid nitrogen for RNA extraction. Transverse sections (8 μm) were performed on a cryostat and stained with hematoxylin and eosin (Sigma, Saint-Quentin, France) or laminin (Dako, Courtaboeuf, France).

Decoy Synthesis and Stability

The decoys were ordered from Eurogentec. Forward and reverse oligonucleotides for decoys were annealed at an equimolar concentration in a final volume of 50 μL and heated at 95°C for 4 min. The ligation was performed with the T4 ligase according to the manufacturer's protocol (New England Biolabs, Evry, France). For decoy stability experiments, 1 μg of pre-annealed decoy was incubated either 30 min at 25°C with 10 U/μL of nuclease S1 (Thermo Scientific, Saint-Aubin, France) or 2 h at 37°C with 160 U/μL of

Table 1. Primers Used in This Study

Gene Symbol	Accession No.	Name	5′ → 3′	Amplicon Length (bp)
Actb	ENSEMBL: ENSMUST00000100497	b-actin_F	CTGTCGAGTCGCGTCCA	223
		b-actin_R	ACCCATTCCCACCATCACAC	
Cyclophilin	GenBank:NM_011149.2	CyclophilinB_F	CCAACGATAAGAAGAAGGGACC	197
		CyclophilinB_R	CTTGATGACACGATGGAACTTG	
Gapdh	GenBank: NM_001289726.1	Gapdh_F	CACCCACCCCAGCAAGGA	98
		Gapdh_R	ATGGGGGTCTGGGATGGAAA	
Gusb	ENSEMBL: ENSMUST00000026613	m_Gusb_F	CGGATCACGATTGCCATCAA	258
		m_Gusb_R	GCCCTGCACAGAAATCCAGT	
Hprt	ENSEMBL: ENSMUSG00000025630	Hprt1_F	TGATCAGTCAACGGGGGACA	199
		Hprt1_R	TCCAACACTTCGAGAGGTCC	
Psma2	GenBank:NM_008944.2	F mPSMA2	AGAGCGCGGTTACAGCTTC	193
		R mPSMA2	CTCCACCTTGTGAACACTCCTT	
Tm7sf4	GenBank:XM_006521519.3	F TM7SF4-2	TATCGGCTCATCTCCTCCAT	98
		R TM7SF4-2	ACTCCTTGGGTTCCTTGCTT	
DUX4	GenBank:XM_017030340.1	F1797	ATGGCCCTCCCGACACCCT	138
		R1906	ATGCCCGGGTACGGGTTCCGCTCAAAG	
TRIM43	GenBank:NM_138800.1	TRIM43_fw	ACCCATCACTGGACTGGTGT	100
		TRIM43_rev	CACATCCTCAAAGAGCCTGA	
ZSCAN4	ENSEMBL: ENSG00000180532	ZSCAN4-fw	GTGGCCACTGCAATGACAA	143
		ZSCAN4-rev	AGCTTCCTGTCCCTGCATGT	

exonuclease III (New England Biolabs, Evry, France), or either during a time course (0, 1, 2, 4, 8, 10, 18, and 24 h) at 37°C with FBS diluted by half. The oligodeoxynucleotides were extracted with phenol and chloroform and examined on a 15% denaturing polyacrylamide gel.

Statistical Analysis

A t test or one-way ANOVA followed by the Newman-Keuls post hoc test were used. Differences were considered statistically different at $p < 0.05$ ($^{*}p < 0.05$, $^{**}p < 0.01$, $^{***}p < 0.001$).

SUPPLEMENTAL INFORMATION

Supplemental Information can be found online at https://doi.org/10.1016/j.omtn.2020.10.028.

ACKNOWLEDGMENTS

V.M, T.V., and J.D. are supported by the National Institute for Health Research Biomedical Research Centre at Great Ormond Street Hospital for Children NHS Foundation Trust and University College London. The views expressed are those of the authors and not necessarily those of the NHS, the NIHR, or the Department of Health. This work was supported by the Wellcome Trust Institutional Strategic Support Fund (grant no. 105604/Z/14/Z), the NIHR GOSH BRC, the FHSD Society (grant no. FSHS-22018-02), and by the Association Française contre les Myopathies (AFM-Telethon, grant no. 22582), France.

AUTHOR CONTRIBUTIONS

J.D. and V.M. conceptualized the study. J.D. and T.V. provided funding. V.M., R.J., A-C.M., C.H., and J.D. performed and analyzed the experiments. C.H. and J.D. performed statistical analysis. The original draft of the article was written by J.D. Review and editing were performed by V.M. and T.V., and the manuscript was approved by all authors. J.D. supervised the project.

DECLARATION OF INTERESTS

A patent named "Treatment of facioscapulohumeral dystrophy" has been filed and includes J.D., V.M. and T.V. as named inventors. The remaining authors declare no competing interests.

REFERENCES

1. Ferreboeuf, M., Mariot, V., Furling, D., Butler-Browne, G., Mouly, V., and Dumonceaux, J. (2014). Nuclear protein spreading: implication for pathophysiology of neuromuscular diseases. Hum. Mol. Genet. *23*, 4125–4133.

2. Wagner, K.R. (2019). Facioscapulohumeral muscular dystrophies. Continuum (Minneap. Minn.) *25*, 1662–1681.

3. Snider, L., Geng, L.N., Lemmers, R.J., Kyba, M., Ware, C.B., Nelson, A.M., Tawil, R., Filippova, G.N., van der Maarel, S.M., Tapscott, S.J., and Miller, D.G. (2010). Facioscapulohumeral dystrophy: incomplete suppression of a retrotransposed gene. PLoS Genet. *6*, e1001181.

4. van der Maarel, S.M., Miller, D.G., Tawil, R., Filippova, G.N., and Tapscott, S.J. (2012). Facioscapulohumeral muscular dystrophy: consequences of chromatin relaxation. Curr. Opin. Neurol. *25*, 614–620.

5. Lemmers, R.J., van der Vliet, P.J., Klooster, R., Sacconi, S., Camaño, P., Dauwerse, J.G., Snider, L., Straasheijm, K.R., van Ommen, G.J., Padberg, G.W., et al. (2010). A unifying genetic model for facioscapulohumeral muscular dystrophy. Science *329*, 1650–1653.

6. Geng, L.N., Yao, Z., Snider, L., Fong, A.P., Cech, J.N., Young, J.M., van der Maarel, S.M., Ruzzo, W.L., Gentleman, R.C., Tawil, R., and Tapscott, S.J. (2012). DUX4 activates germline genes, retroelements, and immune mediators: implications for facioscapulohumeral dystrophy. Dev. Cell *22*, 38–51.

7. Broucqsault, N., Morere, J., Gaillard, M.C., Dumonceaux, J., Torrents, J., Salort-Campana, E., Maues De Paula, A., Bartoli, M., Fernandez, C., Chesnais, A.L., et al. (2013). Dysregulation of 4q35- and muscle-specific genes in fetuses with a short D4Z4 array linked to facio-scapulo-humeral dystrophy. Hum. Mol. Genet. *22*, 4206–4214.

8. Ferreboeuf, M., Mariot, V., Bessières, B., Vasiljevic, A., Attié-Bitach, T., Collardeau, S., Morere, J., Roche, S., Magdinier, F., Robin-Ducellier, J., et al. (2014). DUX4 and DUX4 downstream target genes are expressed in fetal FSHD muscles. Hum. Mol. Genet. *23*, 171–181.

9. Sidlauskaite, E., Le Gall, L., Mariot, V., and Dumonceaux, J. (2020). *DUX4* expression in FSHD muscles: focus on its mRNA regulation. J. Pers. Med. *10*, 73.

10. DeSimone, A.M., Pakula, A., Lek, A., and Emerson, C.P., Jr. (2017). Facioscapulohumeral muscular dystrophy. Compr. Physiol. *7*, 1229–1279.

11. Vanderplanck, C., Ansseau, E., Charron, S., Stricwant, N., Tassin, A., Laoudj-Chenivesse, D., Wilton, S.D., Coppée, F., and Belayew, A. (2011). The FSHD atrophic myotube phenotype is caused by DUX4 expression. PLoS ONE *6*, e26820.

12. Wallace, L.M., Garwick, S.E., Mei, W., Belayew, A., Coppee, F., Ladner, K.J., Guttridge, D., Yang, J., and Harper, S.Q. (2011). *DUX4*, a candidate gene for facioscapulohumeral muscular dystrophy, causes p53-dependent myopathy in vivo. Ann. Neurol. *69*, 540–552.

13. Mitsuhashi, H., Mitsuhashi, S., Lynn-Jones, T., Kawahara, G., and Kunkel, L.M. (2013). Expression of DUX4 in zebrafish development recapitulates facioscapulohumeral muscular dystrophy. Hum. Mol. Genet. *22*, 568–577.

14. Marsollier, A.C., Ciszewski, L., Mariot, V., Popplewell, L., Voit, T., Dickson, G., and Dumonceaux, J. (2016). Antisense targeting of 3′ end elements involved in *DUX4* mRNA processing is an efficient therapeutic strategy for facioscapulohumeral dystrophy: a new gene-silencing approach. Hum. Mol. Genet. *25*, 1468–1478.

15. Chen, J.C., King, O.D., Zhang, Y., Clayton, N.P., Spencer, C., Wentworth, B.M., Emerson, C.P., Jr., and Wagner, K.R. (2016). Morpholino-mediated knockdown of DUX4 toward facioscapulohumeral muscular dystrophy therapeutics. Mol. Ther. *24*, 1405–1411.

16. DeSimone, A.M., Leszyk, J., Wagner, K., and Emerson, C.P., Jr. (2019). Identification of the hyaluronic acid pathway as a therapeutic target for facioscapulohumeral muscular dystrophy. Sci. Adv *5*, eaaw7099.

17. Bosnakovski, D., da Silva, M.T., Sunny, S.T., Ener, E.T., Toso, E.A., Yuan, C., Cui, Z., Walters, M.A., Jadhav, A., and Kyba, M. (2019). A novel P300 inhibitor reverses DUX4-mediated global histone H3 hyperacetylation, target gene expression, and cell death. Sci. Adv *5*, eaaw7781.

18. Oliva, J., Galasinski, S., Richey, A., Campbell, A.E., Meyers, M.J., Modi, N., Zhong, J.W., Tawil, R., Tapscott, S.J., and Sverdrup, F.M. (2019). Clinically advanced p38 inhibitors suppress DUX4 expression in cellular and animal models of facioscapulohumeral muscular dystrophy. J. Pharmacol. Exp. Ther. *370*, 219–230.

19. Le Gall, L., Sidlauskaite, E., Mariot, V., and Dumonceaux, J. (2020). Therapeutic strategies targeting DUX4 in FSHD. J. Clin. Med. *9*, E2886.

20. Zhang, Y., Lee, J.K., Toso, E.A., Lee, J.S., Choi, S.H., Slattery, M., Aihara, H., and Kyba, M. (2016). DNA-binding sequence specificity of DUX4. Skelet. Muscle *6*, 8.

21. Sharma, V., Harafuji, N., Belayew, A., and Chen, Y.W. (2013). DUX4 differentially regulates transcriptomes of human rhabdomyosarcoma and mouse C2C12 cells. PLoS ONE *8*, e64691.

22. Shum, K.T., and Rossi, J.J. (2015). Noncoding oligonucleotides: the belle of the ball in gene therapy. Adv. Genet. *89*, 153–177.

23. Stein, C.A. (1997). Controversies in the cellular pharmacology of oligodeoxynucleotides. Ciba Found. Symp. *209*, 79–89, discussion 89–93.

24. Koziolkiewicz, M., Gendaszewska, E., Maszewska, M., Stein, C.A., and Stec, W.J. (2001). The mononucleotide-dependent, nonantisense mechanism of action of phosphodiester and phosphorothioate oligonucleotides depends upon the activity of an ecto-5′-nucleotidase. Blood *98*, 995–1002.

25. Bosnakovski, D., Xu, Z., Gang, E.J., Galindo, C.L., Liu, M., Simsek, T., Garner, H.R., Agha-Mohammadi, S., Tassin, A., Coppée, F., et al. (2008). An isogenetic myoblast expression screen identifies DUX4-mediated FSHD-associated molecular pathologies. EMBO J. *27*, 2766–2779.

26. Bosnakovski, D., Toso, E.A., Hartweck, L.M., Magli, A., Lee, H.A., Thompson, E.R., Dandapat, A., Perlingeiro, R.C.R., and Kyba, M. (2017). The DUX4 homeodomains mediate inhibition of myogenesis and are functionally exchangeable with the Pax7 homeodomain. J. Cell Sci. *130*, 3685–3697.

27. Banerji, C.R.S., Panamarova, M., Hebaishi, H., White, R.B., Relaix, F., Severini, S., and Zammit, P.S. (2017). PAX7 target genes are globally repressed in facioscapulohumeral muscular dystrophy skeletal muscle. Nat. Commun. *8*, 2152.

28. Banerji, C.R.S., and Zammit, P.S. (2019). PAX7 target gene repression is a superior FSHD biomarker than DUX4 target gene activation, associating with pathological severity and identifying FSHD at the single-cell level. Hum. Mol. Genet. *28*, 2224–2236.

29. Zammit, P.S., Relaix, F., Nagata, Y., Ruiz, A.P., Collins, C.A., Partridge, T.A., and Beauchamp, J.R. (2006). Pax7 and myogenic progression in skeletal muscle satellite cells. J. Cell Sci. *119*, 1824–1832.

30. Arnett, A.L., Konieczny, P., Ramos, J.N., Hall, J., Odom, G., Yablonka-Reuveni, Z., Chamberlain, J.R., and Chamberlain, J.S. (2014). Adeno-associated viral (AAV) vectors do not efficiently target muscle satellite cells. Mol. Ther. Methods Clin. Dev. *1*, 14038.

31. Novak, J.S., Hogarth, M.W., Boehler, J.F., Nearing, M., Vila, M.C., Heredia, R., Fiorillo, A.A., Zhang, A., Hathout, Y., Hoffman, E.P., et al. (2017). Myoblasts and macrophages are required for therapeutic morpholino antisense oligonucleotide delivery to dystrophic muscle. Nat. Commun. *8*, 941.

32. Tomita, T., Kunugiza, Y., Tomita, N., Takano, H., Morishita, R., Kaneda, Y., and Yoshikawa, H. (2006). E2F decoy oligodeoxynucleotide ameliorates cartilage invasion by infiltrating synovium derived from rheumatoid arthritis. Int. J. Mol. Med. *18*, 257–265.

33. Wu, J., Sabirzhanov, B., Stoica, B.A., Lipinski, M.M., Zhao, Z., Zhao, S., Ward, N., Yang, D., and Faden, A.I. (2015). Ablation of the transcription factors E2F1-2 limits neuroinflammation and associated neurological deficits after contusive spinal cord injury. Cell Cycle *14*, 3698–3712.

34. Liu, M., Wang, F., Wen, Z., Shi, M., and Zhang, H. (2014). Blockage of STAT3 signaling pathway with a decoy oligodeoxynucleotide inhibits growth of human ovarian cancer cells. Cancer Invest. *32*, 8–12.

35. Zhang, Q., Hossain, D.M., Duttagupta, P., Moreira, D., Zhao, X., Won, H., Buettner, R., Nechaev, S., Majka, M., Zhang, B., et al. (2016). Serum-resistant CpG-STAT3 decoy for targeting survival and immune checkpoint signaling in acute myeloid leukemia. Blood *127*, 1687–1700.

36. Morishita, R., Sugimoto, T., Aoki, M., Kida, I., Tomita, N., Moriguchi, A., Maeda, K., Sawa, Y., Kaneda, Y., Higaki, J., and Ogihara, T. (1997). In vivo transfection of cis element "decoy" against nuclear factor-κB binding site prevents myocardial infarction. Nat. Med. *3*, 894–899.

37. Kim, K.H., Lee, W.R., Kang, Y.N., Chang, Y.C., and Park, K.K. (2014). Inhibitory effect of nuclear factor-κB decoy oligodeoxynucleotide on liver fibrosis through regulation of the epithelial-mesenchymal transition. Hum. Gene Ther. *25*, 721–729.

38. Sen, M., Thomas, S.M., Kim, S., Yeh, J.I., Ferris, R.L., Johnson, J.T., Duvvuri, U., Lee, J., Sahu, N., Joyce, S., et al. (2012). First-in-human trial of a STAT3 decoy oligonucleotide in head and neck tumors: implications for cancer therapy. Cancer Discov. *2*, 694–705.

39. Boutin, S., Monteilhet, V., Veron, P., Leborgne, C., Benveniste, O., Montus, M.F., and Masurier, C. (2010). Prevalence of serum IgG and neutralizing factors against adeno-associated virus (AAV) types 1, 2, 5, 6, 8, and 9 in the healthy

population: implications for gene therapy using AAV vectors. Hum. Gene Ther. *21*, 704–712.

40. Colella, P., Ronzitti, G., and Mingozzi, F. (2017). Emerging issues in AAV-mediated *in vivo* gene therapy. Mol. Ther. Methods Clin. Dev. *8*, 87–104.

41. Bertin, B., Veron, P., Leborgne, C., Deschamps, J.Y., Moullec, S., Fromes, Y., Collaud, F., Boutin, S., Latournerie, V., van Wittenberghe, L., et al. (2020). Capsid-specific removal of circulating antibodies to adeno-associated virus vectors. Sci. Rep. *10*, 864.

42. Leborgne, C., Barbon, E., Alexander, J.M., Hanby, H., Delignat, S., Cohen, D.M., Collaud, F., Muraleetharan, S., Lupo, D., Silverberg, J., et al. (2020). IgG-cleaving endopeptidase enables in vivo gene therapy in the presence of anti-AAV neutralizing antibodies. Nat. Med. *26*, 1096–1101.

43. Mariot, V., Roche, S., Hourdé, C., Portilho, D., Sacconi, S., Puppo, F., Duguez, S., Rameau, P., Caruso, N., Delezoide, A.L., et al. (2015). Correlation between low FAT1 expression and early affected muscle in facioscapulohumeral muscular dystrophy. Ann. Neurol. *78*, 387–400.

44. Bustin, S.A., Benes, V., Garson, J.A., Hellemans, J., Huggett, J., Kubista, M., Mueller, R., Nolan, T., Pfaffl, M.W., Shipley, G.L., et al. (2009). The MIQE guidelines: minimum information for publication of quantitative real-time PCR experiments. Clin. Chem. *55*, 611–622.